Applied Thermal Engineering 146 (2019) 39–44

Contents lists available at ScienceDirect

Applied Thermal Engineering

journal homepage: www.elsevier.com/locate/apthermeng

Research Paper

Mixing of rarefied gases in T-shape micromixers

Mubashir Hussain*, Thorsten Pöschel, Patric Müller

Institute of Multiscale Simulation, University of Erlangen-Nürnberg, Germany

HIGHLIGHTS

- Wall characteristics have significant effect on gas mixing.
- Mixing length is predicted by means of Kinetic theory.
- Diffusion dominates in mixing of gases with different molecular mass.
- Ratio of molecular masses and inlet velocity effect gas mixing significantly.

ARTICLE INFO

Keywords:
Mixing
T-shape
Discrete simulation Monte-Carlo
Simulation
Rarefied flows

ABSTRACT

We study the mixing of rarefied gases in a T-shape micromixer by means of fully three-dimensional Monte-Carlo direct simulations. In contrast to previous 2D-results, the characteristics of the channel walls (thermal or specular) have significant effect on the mixing efficiency. For the 3D case, we characterize the mixing efficiency in dependence on temperature and mass density of the gases. Based on kinetic theory arguments, we develop a theoretical model in good agreement with the simulation results. In particular, the theoretical prediction of system size scaling agrees well with the simulation.

1. Introduction

T-shape micromixers are of great importance for various microfluidic devices [9]. In many of these devices such as microreactors, microturbines or micropumps, the efficiency of mixing in T-shape micromixers is critical for the efficiency of the whole device [8]. The process of mixing in microfluidic devices differs from mixing of gases in macroscopic systems since the flow through microfluidic channels is nearly laminar due to their small characteristic size [15]. Moreover, the residence time of gas molecules in the channels of microfluidic devices is typically short compared to the mean free time of the gas molecules, that is, to achieve the desired functionality of a microreactor, the gases must be mixed within a short period of time. For both reasons, mixing of gases in microfluidic devices is challenging.

Numerical simulations are valuable tools in order to understand the complex process of micromixing and subsequently design optimized microfluidic devices. In typical applications, the flow of gases in microchannels is rarefied, that is, the mean free path of the gas molecules is comparable to the dimensions of the microchannel [8], expressed by the Knudsen number $\mathrm{Kn} \gtrsim 1$. Therefore, the continuum assumption underlying Navier-Stokes based CFD is violated such that traditional CFD may be problematic for the simulation of microfluidic systems, e.g. [3,4,2,17]. CFD simulations are therefore only feasible for relatively large systems. For instance, the T-shape micromixers considered in the CFD study of [7] are 500 times larger then the T-mixer considered here. Similarly, an interesting study on the effect of fluid velocity on mixing in serpentine micromixers is conducted by [11] by means of CFD simulations. The length and width of their micromixer is approximately 5 mm and 0.3mm, respectively, which is once again quiet large as compared to the dimensions of the T-mixer considered in this study. Therefore, it was argued that computations of the gas dynamics on the molecular level are required for the simulation of micromixing processes [10]. While the molecular dynamic simulation of the micromixer is far from being feasible due to the enormous number of gas molecules, in this paper we employ a mesoscopic simulation method and show that mesoscopic simulations are able to describe the mixing process while being numerically feasible at the same time.

Unlike fluid dynamical approaches, kinetic descriptions on the level of the Boltzmann equation do not rely on the continuum assumption and, thus, do not suffer from the breakdown of traditional fluid dynamics in the Knudsen regime. Direct Simulation Monte Carlo (DSMC) [1] is a numerical simulation method to solve the Boltzmann equation using the approach of quasi-particles. While delivering reliable results, even in systems where the continuum assumption is not justified, DSMC

* Corresponding author.
E-mail address: mubashir.hussain@fau.de (M. Hussain).

https://doi.org/10.1016/j.applthermaleng.2018.09.090
Received 14 June 2018; Received in revised form 13 September 2018; Accepted 22 September 2018
Available online 24 September 2018
1359-4311/

Nomenclature

Latin symbols

D	diffusion coefficient (m^2/s)
l	number of cells in a cross-section
M	molar mass (g/mol)
n	number density ($1/m^3$)
P	pressure (Pa)
R	gas constant (J/mol K)
s	scaling factor
T	temperature (K)
t	time (s)
v	velocity (m/s)
w	main channel width (μm)
x^M	mixing length (μm)

Subscripts

i	integer index
a	specie a
b	specie b
Kn	Knudsen
mol	molecular

Greek symbols

α	dimensionless weight $\in [0, 1]$
β	dimensionless constant of proportionality
δ	distance (m)
σ	collision diameter (Å)
ψ	number density fraction
ξ	mixing intensity
Ω	temperature dependent collision integral

Abbreviations

CFD	Computational Fluid Dynamics
DSMC	Direct Simulation Monte-Carlo
NTC	No time counter

methods are significantly more computer time costly than CFD methods. Therefore, by now, almost all MC direct simulations of gases in small geometries have been performed for two-dimensional systems [18,15,8,13].

In this work we apply fully three-dimensional DSMC for the simulation of mixing rarefied gases in a T-shape micromixer. We show that the characteristics of the channel walls (thermal or specular) have significant effect on the mixing efficiency which is in contrast to earlier two-dimensional simulations. The simulation results deliver the dependence of the mixing efficiency as a function of temperature and density in good agreement with the kinetic theory. Finally, we develop a scaling relation which allows to generalize the simulation results.

2. Model description

2.1. T-shape geometry

The T-shape micromixer of overall volume $16.8\,\mu m^3$ is sketched in Fig. 1. Gases A and B enter the system at both sides of the inlet channel, start interacting near the contact of inlet and main channel and flow downstream while mixing towards the outlet. Both channels have rectangular cross-section of the size $(1 \times 1)\,\mu m^2$ (inlet) and $(1.2 \times 1)\,\mu m^2$ (main). The inlet and the main parts of the microchannel are $4.8\,\mu m$ and $10\,\mu m$ long, respectively.

2.2. Direct Simulation Monte-Carlo (DSMC)

Direct Simulation Monte Carlo [1] is a numerical scheme to solve the Boltzmann equation in order to obtain the time and space dependent velocity distribution function of the gas molecules. With 'velocity distribution function' we mean here the differential probability distribution of the velocities, that is, the probability density. DSMC uses quasi-particles representing probability quanta. Similar as gas molecules, these quasi-particles interact through collisions, thus transferring momenta. The interaction rules follow from kinetic gas theory, for a simple introduction see, e.g., [12]. In this sense, DSMC may be considered as a *particle-based* simulation method with the only difference that the particles are interpreted as probability quanta rather than molecules. The result of a DSMC simulation is the velocity distribution function from which subsequently the macroscopic field variables such as mass density, velocity, and temperature of the gas are obtained as its first moments. Frequently, the pressure is then computed from temperature and density through the equation of state of the gas.

In this study, we have used an in-house, highly efficient C++ code of 3D DSMC for simulating the gas flow. The code is parallelized in shared and distributed memory and is capable of simulating gas flow in arbitrarily complex geometries. For the simulation, we apply the no-time-counter (NTC) scheme [1] to enhance computational efficiency. The code has been extensively tested against benchmark problems in [14]. Moreover, quasi-2D simulations have been performed by considering the width of the third dimension equal to the diameter of a gas

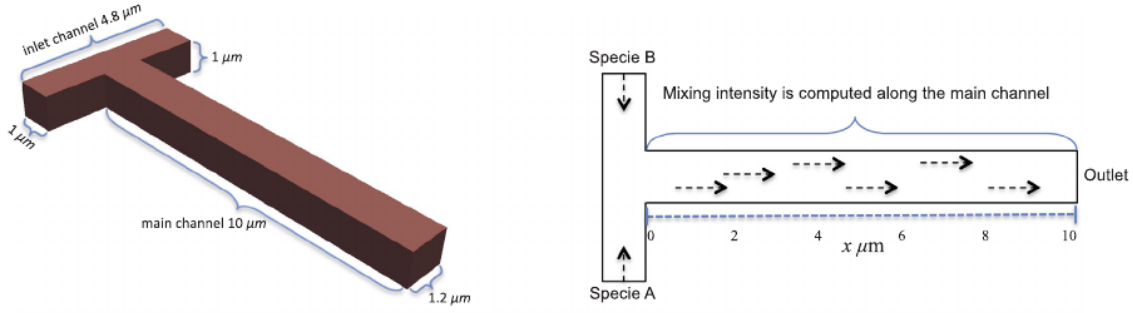

(a) Dimensions of the T-shape mixer (b) Direction of the gas flow

Fig. 1. Description of the T-shape geometry.

molecule and assuming periodic boundary conditions in this 3rd direction. The results of the quasi-2D simulations were compared to the 2D gas flow simulation results of [13] and found in excellent agreement. The details of the simulation software are given in [14].

We start with a homogeneous distribution of the quasi-particles over the simulation domain and their velocities are chosen according to a Maxwell distribution. Each DSMC time step comprises a *streaming* step and a *collision* step. In the streaming step the particles are propagated for a given time interval according to their current velocity. During the collision step, random pairs of particles are chosen in each cell of the simulation grid to perform binary hard sphere collisions. Moreover, inlets and outlet are modeled through Dirichlet boundary conditions for pressure, temperature and flow velocity [6]. The channel boundaries are modeled either as specular or thermal walls, specified in the text below.

For the computation of the hydrodynamical fields we used a total of 2.625×10^5 cubical coarse graining volumes of size $0.04\,\mu\text{m}$. The gas flow is driven by the inlet-outlet pressure difference, where the pressure at the inlets and outlet are chosen to be $10^5\,\text{Pa}$ and $0\,\text{Pa}$ (vacuum), respectively, in all simulations. The inlet and outlet pressures are directly related to the density/number of particles that enter into the system in unit time. Therefore, by setting inlet pressure 10^5 Pa, we mean that gas molecules enter into the system at a density corresponding to this pressure with a certain average velocity specified separately. Moreover, 0 pressure at the outlet means that no gas molecule can enter into the system from the outlet i.e. no back-mixing is possible. In DSMC, the time step is limited by the mean free time of the molecules; in all simulations we used 2×10^{-11} s which is well below the limit. In the simulations, all data are taken after disregarding the first 2×10^{-6} s (10^5 time steps), when the system assumed its stationary state. Data are averaged over the period 10^{-6} s (5×10^4 time steps) to improve the statistics.

2.3. Mixing length

There are several methods to quantify the degree of mixing globally, e.g. [18,15,7,3]. Here, however, we need a measure of the homogeneity operating locally to quantify the degree of mixing of the gas flow alongside the micromixer. For a mixture of gases a and b, we quantify the degree of mixing in a cross sectional slice along the main channel of the T-mixer by

$$\xi_a = \sqrt{\frac{\sum_{i=1}^{l} (\psi_{a,i}(x) - \psi_a)^2}{l\psi_a^2}}, \tag{1}$$

where

$$\psi_{a,i} = \frac{n_{a,i}}{n_{a,i} + n_{b,i}} \tag{2}$$

is the relative concentration of quasi-particles of type a with number density n in the coarse-graining lattice site i. The sum in Eq. (1) is performed over all cells $i = 1..l$, corresponding to the current cross sectional slice. The average a-population of these sites is given by

$$\psi_a = \frac{\sum_{i=1}^{l} n_{a,i}}{\sum_{i=1}^{l} (n_{a,i} + n_{b,i})}, \tag{3}$$

In our simulations, each slice consists of $l = 750$ coarse-graining cells of volume $(0.04 \times 1.2 \times 1)\,\mu\text{m}^3$. For the example of perfect mixing, of a binary mixture with $n_a = n_b$, obviously, we obtain $\psi_{a,i} = 0.5$ and $\xi_a = 0$. If the gases are fully separated, we have $\xi_a = 1$.

For the geometry sketched in Fig. 1, we expect the degree of mixing to increase along the main channel towards the outlet, thus ξ_a to be a decreasing function, up to fluctuations. Therefore. we may define a mixing length, $x^M(\xi_a^{\text{thr}})$, as the downstream position when ξ_a drops below a certain threshold, ξ_a^{thr} at which we consider the gas sufficiently mixed.

3. Mixing of gases with similar molecular mass

We consider the mixing of N_2 and CO at inlet and outlet pressure set to $10^5\,\text{Pa}$ and $0\,\text{Pa}$, respectively. The gases have nearly identical molecular mass, $4.65 \times 10^{-26}\text{kg}$.

3.1. Influence of wall characteristics

We consider two types of walls, specular walls and thermal walls. When a quasi particle collides with a specular wall, it is reflected geometrically (corresponding to ideally smooth walls). When it collides with a thermal wall, it is re-injected diffusively, according to the temperature of the wall. Moreover, the gas inlet velocity is taken to be 300 m/s for this set of simulations which means that the gas molecules entering into the system have Maxwell distribution of velocity with an average of 300 m/s. It should be noted that the pressure at the inlets is correlated to the density of the inlet gas. This setup means that by taking into account pressure at the inlets, a certain number of particles is created in each time step to enter into the T-mixer with an average velocity of 300 m/s. This option to set velocity to the gas separately is an exclusive feature of our code and can be very helpful in understanding the gas dynamics, for example, in jet flows. The temperature of both gases and thermal walls is 300 K. Fig. 2 shows the degree of mixing, ξ, defined in Eq. (1) as a function of the downstream position along the main channel, x, for all combinations (main channel, inlet channel) $\times$ (specular, thermal).

While the characteristics of the walls of the inlet channel have only minor effect on the efficiency of the mixer, the walls of the main channel are of great importance: In the case of thermal main walls, the mixing length $x^{\text{M}} \approx 3\,\mu\text{m}$ is found for $\xi_a^{\text{thr}} = 0.01$, that is, only 3 μm after the beginning of the main channel, the gas is already nearly perfectly mixed. For the case of specular main channel walls, mixing is much less efficient. Therefore, thermal main walls are required for optimal mixing efficiency. The specific value of the wall temperature is not crucial. Even at small temperature, thermal walls lead to fluctuations which break up the laminar downstream flow and allow, thus, for better mixing. This observation is interesting because previous 2-dimensional DSMC simulations of T-micromixer under almost identical operation conditions [15] show that the influence of the wall conditions is unimportant for the mixing efficiency. Just the opposite: in [15] the mixing length is found slightly smaller (corresponding to more efficient mixing) for the case of specular walls. The difference between the earlier 2-dimensional results [15] and our 3-dimensional results shown in Fig. 2 can be understood from the weaker influence of walls in 2d and

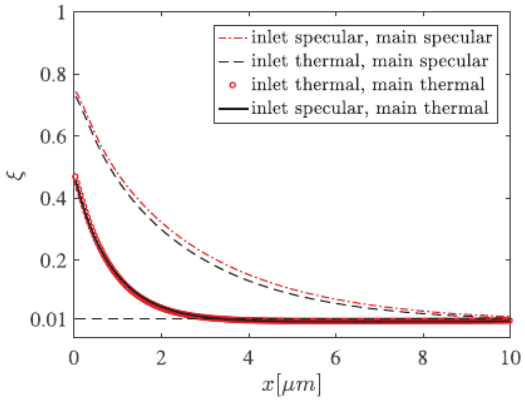

Fig. 2. Effect of wall characteristics of a T-shape micromixer. Degree of mixing, ξ, (see Eq. (1)) as a function of the downstream position along the main channel, x, for the combinations of boundary conditions.

3d and from additional fluctuational velocity and concentration gradients along the third dimension which are disregarded in 2d simulations [7].

The overall pressure drop along the mixer is shown in Fig. 3. While the boundary conditions of the inlet channel do not significantly influence the mixing properties, the difference of pressure drop is noticeable. Nevertheless the overall pressure drop is primarily determined by the main channel walls. Therefore, if thermal main walls are chosen to achieve a high mixing efficiency, the additional pressure drop due to thermal inlet walls is negligible.

It can be noticed that the pressure along the channel and especially at the start of the main channel i.e. at $x = 0$ is higher as compare to the inlet pressure. The reason is that the walls of the micro-channel create resistance in the flow of the gas which gives rise to an increase in pressure in the channel. This resistance and thus the pressure is much higher in case of thermal walls as compare to specular walls which can be observed in Fig. 3. Further, $x = 0$ is the location where gas streams from both inlets collide. Therefore, apart from wall effects, an additional pressure is created by the chaotic interactions of both gases at this location which gives rise to even higher local pressure.

3.2. In uence of the gas temperature on the mixing e ciency

Intuitively it is expected, that increasing gas temperature would increase the mixing efficiency as well, because higher temperature implicates more fluctuations in the system which, in turn, facilitates mixing. Fig. 4 (circles) shows the corresponding simulations results. Here we simulated thermal walls and varied the temperature of the gases at the inlet as well as the temperature of the walls without assigning any superimposed velocity to the inlet gas. As expected, the mixing length decreases monotonically with temperature.

Quantitatively, the relation between temperature and mixing length can be understood as follows: Consider two gases flowing along a channel in the laminar regime. In this case, mixing take place predominantly due to diffusion, that is, the mean square displacement of the molecules increases proportional to time: $\delta^2 \propto Dt$, where D is the diffusion coefficient. Therefore, the width of the mixing zone grows like $\sqrt{Dt}$. Since, on average, a molecule covers the distance of $\delta \propto \sqrt{Dt}$ during the time interval t. Complete mixing is achieved, when the width of the mixing zone approaches the channel width, w, that is at time $t = \beta w^2/D$, where β is a dimensionless constant of proportionality. Consequently, the mixing length reads

$$x^{\mathrm{M}}(w,\ T)\ = vt = \beta v\frac{w^2}{D}, \tag{4}$$

where v, is the stream velocity of the gas. For an estimate for the diffusion coefficient, D, we have to keep in mind that the considered T-mixer is of intermediate size where both mechanisms of diffusion may be relevant: Knudsen diffusion where the mean free path of the molecules is limited by the system size and ordinary molecular diffusion. In the Knudsen regime, the diffusion coefficient derived from kinetic theory of gases reads [5]

$$D_{\mathrm{Kn}} = \frac{w}{3}\sqrt{\frac{8RT}{\pi M}}, \tag{5}$$

where R is the gas constant, M is the molar mass of the gases (almost equal for N_2 and CO, see Table 1). For ordinary molecular diffusion, Chapman-Enskog theory [16] delivers

$$D_{\mathrm{mol}} = \frac{AT^{\frac{3}{2}}\sqrt{\frac{1}{M_{\mathrm{N_2}}} + \frac{1}{M_{\mathrm{CO}}}}}{P\sigma^2\Omega}. \tag{6}$$

Here, A is an empirical constant, P is the pressure, σ is the average collision diameter, and Ω is the temperature dependent collision integral. The values of these parameters specified for our problem are summarized in Table 1.

For mesoscopic systems, both diffusion mechanisms contribute, therefore, we use the effective coefficient of diffusion [20]

$$\frac{1}{D} = \frac{\alpha}{D_{\mathrm{mol}}} + \frac{1-\alpha}{D_{\mathrm{Kn}}}, \tag{7}$$

where $\alpha \leq 1$ weights the alternative diffusion mechanisms. Inserting Eq. (7) into Eq. (4), we obtain the mixing length

$$x^{\mathrm{M}}(w,\ T) = \beta v w^2\left(\alpha\frac{P\sigma^2\Omega}{AT^{\frac{3}{2}}\sqrt{\frac{1}{M_{\mathrm{N_2}}} + \frac{1}{M_{\mathrm{CO}}}}} + (1-\alpha)\frac{3}{w}\sqrt{\frac{\pi M_{\mathrm{CO}}}{8RT}}\right), \tag{8}$$

(see Fig. 4, dashed line). The free parameters, α and β, are fitted to the corresponding simulation results (circles in Fig. 4), the average streaming velocity of the gases in main channel is $336\ \mathrm{m/s}$ in the simulation. The value of β is found to be 0.235, whereas, the value of $\alpha = 0.809$ indicate that both, Knudsen and molecular diffusion play a role in mixing with molecular diffusion being dominant. It should be noted that by increasing the temperature from $200\ \mathrm{K}$ to $500\ \mathrm{K}$, the stream velocity as well as the speed of sound increases from 259 m/s to 402 m/s and 254 m/s to 407 m/s, respectively. However, the Mach number remains higher then 0.3 resulting in compressible flow under all conditions.

The mathematical expression (8) for the mixing length takes into account both diffusion coefficients i.e. molecular diffusion and Knudsen diffusion. It can be considered as a normalized weighted sum of both diffusion coefficients. The fitting parameter α represents the normalized weight. If one diffusion phenomenon is dominant then the other diffusion coefficient vanishes because α will be very close to either 0 or 1. However, if we are in a transition regime then both diffusion coefficients play a role in the mixing of gases and α will take a value between 0 and 1. This is shown in Fig. 4. From the good agreement of the DSMC data and Eq. (8) we conclude that the proposed theory captures the essential features of the problem.

3.3. Scaling relation for the mixing length

To study the dependence of the mixing length on the system size, we repeat the simulation presented in Section 3.2 for $T = 300\ \mathrm{K}$ but with the whole geometry scaled by a factor $s = (0.3,\ ...,\ 30)$, that is we study T-mixers with channel width in the range $(0.3...30)\,\mu\mathrm{m}$ while all remaining parameters are kept the same. Consequently, the number of molecules and, thus, the number of simulated quasi-particles grows $\sim s^3$.

Fig. 5 show the mixing lengths as a function of the scaling factor. The best fit of the DSMC data to Eq. (8) is obtained for $\alpha = 2.243 \times 10^{-13}$ and $\beta = 0.14$. Since $\alpha \approx 0$, Knudsen diffusion dominates and from Eq. (8) we obtain that the mixing length scales linearly with the scaling

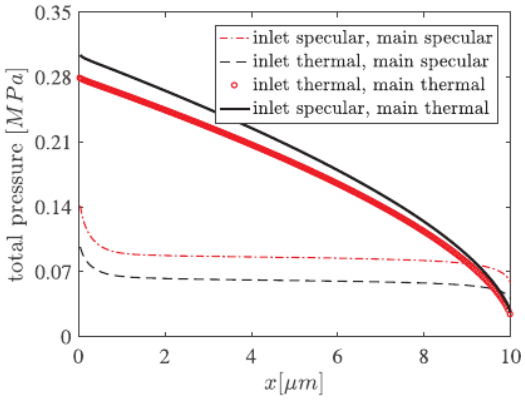

Fig. 3. Comparison of average pressure drop in the main part of T-mixer.

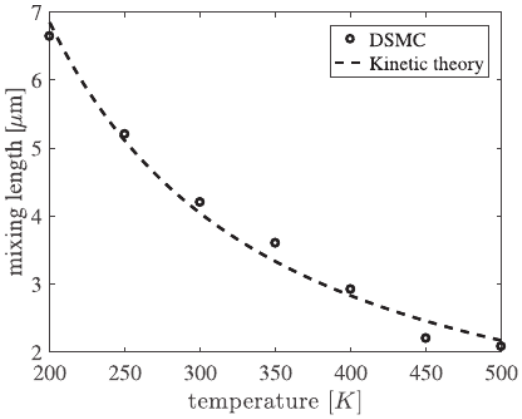

Fig. 4. Influence of temperature on the mixing length. DSMC simulation (circles) and kinetic theory (dashed line) according to Eq. (8) with $\alpha = 0.809$, $\beta = 0.235$.

Table 1
Problem-specific parameters.

Parameter	Value	Unit
A	1.858×10^{-3}	atm Å^2 cm^2 $\sqrt{\frac{g}{mol}}$/K$^{3/2}$s
$M = M_{CO} = M_{N_2}$	28.01	g/mol
R	8.3144	J/mol K
T	200–500	K
w	0.3–30	μm
σ	3.7	Å
Ω	0.9	–

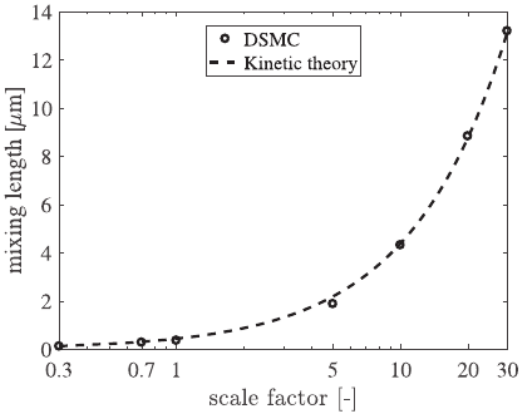

Fig. 5. Mixing length as a function of the scaling factor. Points: DSMC simulation results for $v = 50\,\frac{m}{s}$; line: prediction from kinetic theory, Eq. (8).

factor, $x^M \propto s$ which is in good agreement with the numerical data. The same linear behavior, $x^M \propto s$, is also observed when the Knudsen number is kept constant while scaling the system size, thus, x^M does not depend on the Knudsen number as long as the flow is in the Knudsen regime. Fig. 5 can also be correlated to Knudsen number since $Kn = \lambda/h$, where λ and h are the mean free path and the characteristic length, respectively. In our setup the characteristic length h is equal to the scaling factor. The interesting fact we noticed is that even in case of relatively low Knudsen numbers, the Knudsen diffusion coefficient can still give a good fit to predict an approximate mixing length in T-mixers.

Qualitatively, the mixing behavior is in good agreement with the 2D simulation results by Le and Hassan [8], however, the mixing length found in our three-dimensional simulations is almost 3 times larger. Again, we see that the third dimension must not be neglected for the phenomenon of micro-mixing.

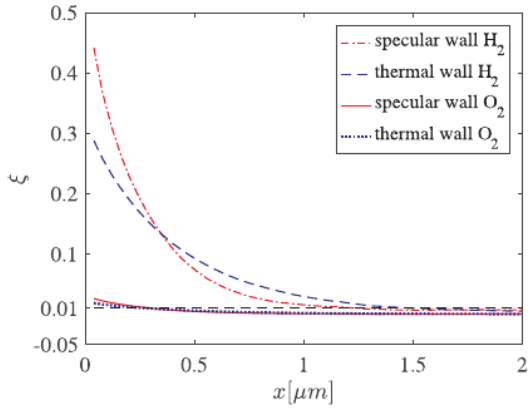

Fig. 6. Effect of wall characteristics (specular and thermal) of a T-shape micromixer on gases with different molecular mass. Degree of mixing, ξ, (see Eq. (1)) as a function of the downstream position along the main channel, x.

4. Mixing of gases of di erent molecular mass

Many practical applications require the mixing of gases of different densities, e.g., non-premixed combustion which is typically carried out in microcombustors by mixing oxygen and hydrocarbon gases [19]. Here, we consider the mixing of H_2 and O_2 of molecular masses 3.34×10^{-27} kg and 5.313×10^{-26} kg in a T-mixer. Inlet pressure is 10^5 Pa, the inlet gas velocity 300 m/s, and the temperature of both gases 300 K.

It can be observed in Fig. 6 that both gas species, irrespective of the wall condition, are adequately mixed within 1.5 μm of distance after entering into the main channel. This means that in case of different mass densities of gas species, the diffusion of molecules significantly dominates over wall characteristics during mixing process. Additionally, it can further be noted in Fig. 6 that O_2 is distributed homogeneously quite earlier as compare to H_2. It is to be noted that Fig. 6 is plotted only until 2 μm to highlight the mixing length. We noticed some non equilibrium effects for the lighter gas i.e. H_2 at the end of the channel due to the vacuum boundary condition. However, our focus here is to determine the mixing length of the gases therefore we omit any further details regarding non-equilibrium effects due to the boundary conditions.

In order to understand the mixing behavior of gases with different molecular mass, we have to recall that the mixing intensity, Eq. (1), characterizes the *homogeneity* of a gas in a cross sectional volume of the channel. It, however, does not provide information about the concentrations in the mixing. For gases with identical densities such as, e.g., CO and N_2, we expect the same amount of molecules of either gas per unit volume. This is, however, not true for gases of different densities, Fig. 7.

To understand the behavior, we first consider the case when both gases, H_2 and O_2, enter the system at inlet gas velocity 300 ms^{-1} as in the preceding sections. In this case, the majority of all molecules in the main channel are O_2 molecules since O_2 molecules arrive at much larger momentum due to their mass. Thus, the O_2 molecules penetrate far into the H_2 inlet channel and hinder the H_2 molecules from entering the main channel, see Fig. 8. This behavior changes when the inflow velocity is reduced, since then the larger diffusivity of the H_2 molecules dominates. In the case of vanishing inflow velocity, H_2 propagates far into the O_2 inlet channel due to its higher diffusivity and, thus, tend to block the O_2 molecules.

Therefore, we conclude that the mixing behavior of gases of different molecular mass is dominated by the inlet stream velocities. Further, gases of different molecular mass are found to be well mixed at

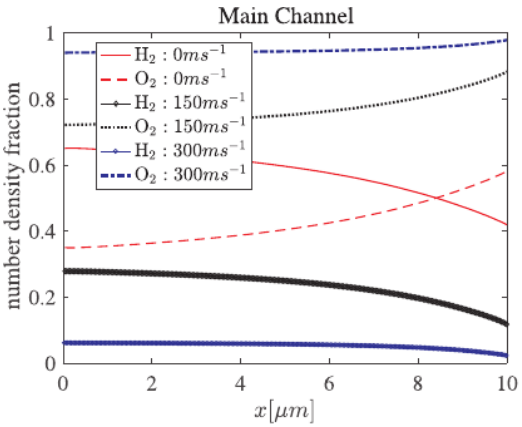

Fig. 7. Number density fraction of H_2 and O_2 as a function of the downstream position in the main channel for various values of the inflow velocity.

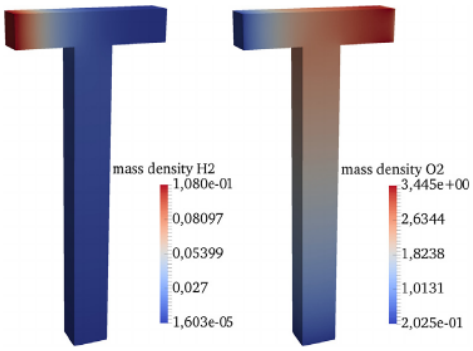

Fig. 8. Mass density of H_2 and O_2 in a T-shape micromixer with an inflow velocity of 300ms^{-1}.

all inlet velocities considered in this study. However, the quantity or ratio of one gas specie mixed with the other is significantly affected by changing the velocity. Other effects such as wall characteristics (specular or thermal) are less important. Consequently, the mixing ratio of the gases can be controlled by the inlet gas velocities to great extend.

5. Summary

By now, all available three-dimensional simulations of T-shape micromixers have been performed by means of classical, lattice-based simulations of the hydrodynamical simulations on the Navier-Stokes level. This approach is, however, problematic because in mesoscopic systems the underlying continuum assumptions may be violated. In order to assure the validity of the hydrodynamic approach, much larger systems were simulated and the results were downscaled to the true dimensions of the micromixer [7]. In contrast, as a particle-based method, direct simulation Monte Carlo (DSMC) does not rely on the continuum assumptions, however, because of its high computational cost so far, DSMC has only been applied to two-dimensional systems.

Here, we studied the efficiency of T-shape micromixers for mixing rarefied gases by means of *three-dimensional* mesoscopic DSMC simulations. From the results we concluded that two-dimensional simulations are not sufficient to understand the behavior of micromixers. In particular, we have shown that the characteristics of the channel walls may have significant influence on the mixing efficiency. This is in sharp contrast to the results of previous two-dimensional simulations. Further we found that the mixing length increases linearly with the system size and decreases with increasing temperature of the mixed gases like $T^{-3/2}$. Both results are in good agreement with kinetic theory. The scaling relation for the system size allows to extrapolate simulation data to larger, technically relevant systems which would not be accessible directly by DSMC.

Finally, we investigated the mixing of gases of different molecular mass, such as H_2 and O_2. Here, the mixing properties are predominantly influenced by the ratio of the molecular masses and the ratio of the inflow streaming velocity of the gases.

Acknowledgments

The authors gratefully acknowledge the support of the Cluster of Excellence “Engineering of Advanced Materials” at the University of Erlangen-Nuremberg, which is funded by the German Research Foundation (DFG) within the framework of its “Excellence Initiative”. The first author is further thankful to Sebastian Mühlbauer and Prapanch Nair for their helpful comments and suggestions.

Appendix A. Supplementary material

Supplementary data associated with this article can be found, in the online version, at https://doi.org/10.1016/j.applthermaleng.2018.09.090.

References

[1] G.A. Bird, Molecular Gas Dynamics and the Direct Simulation of Gas Flows, Clarendon, Oxford, UK, 1994.
[2] D. Bothe, A. Lojewski, H.-J. Warnecke, Fully resolved numerical simulation of reactive mixing in a T-shaped micromixer using parabolized species equations, Chem. Eng. Sci. 66 (2011) 6424–6440.
[3] D. Bothe, C. Stemich, H.-J. Warnecke, Fluid mixing in a T-shaped micro-mixer, Chem. Eng. Sci. 66 (2006) 2950–2958.
[4] D. Bothe, C. Stemich, H.-J. Warnecke, Computation of scales and quality of mixing in a T-shaped microreactor, Comp. Chem. Eng. 32 (2008) 108–114.
[5] S. Chapman, T.G. Cowling, D. Burnett, The Mathematical Theory of Non-uniform Gases: An Account of the Kinetic Theory of Viscosity, Thermal Conduction, and Diffusion in Gases, Cambridge University Press, 1970.
[6] A.L. Garcia, W. Wagner, Generation of the maxwellian inflow distribution, J. Comput. Phys. 217 (2) (2006) 693–708.
[7] D. Gobby, P. Angeli, A. Gavriildis, Mixing characteristics of T-type microfluidic mixers, J. Micromech. Microeng. 11 (2001) 126–132.
[8] M. Le, L. Hassan, DSMC simulation of gas mixing in T-shape micromixer, Appl. Therm. Eng. 27 (2007) 2370–2377.
[9] C.-Y. Lee, C.-L. Chang, Y.-N. Wang, L.-M. Fu, Microfluidic mixing: a review, Int. J. Mol. Sci. 12 (2011) 3263–3287.
[10] M. Losey, R. Jackman, S. Firebaugh, M. Schmidt, K. Jensen, Design and fabrication of microfluidic devices for multiphase mixing and reaction, J. Microelectromech. Syst. 11 (6) (2002) 709–717.
[11] Z.M. Malecha, K. Malecha, Numerical analysis of mixing under low and high frequency pulsations at serpentine micromixers, Chem. Process Eng. 35 (2014) 369–385.
[12] T. Pöschel, T. Schwager, Computational Granular Dynamics: Models and Algorithms, Springer-Verlag, Berlin, Heidelberg, 2005.
[13] M. Reyhanian, C. Croizet, R. Gatignol, Numerical analysis of the mixing of two gases in a microchannel, Mech. Ind. 14 (2013) 453–460.
[14] S. Strobl, Mesoscopic Particle-based Complex Geometries (Ph.D. thesis), Friedrich-Alexander-Universität Erlangen-Nürnberg, 2017.
[15] M. Wang, Z. Li, Gas mixing in microchannels using the direct simulation monte carlo method, Int. J. Heat Mass Transf. 49 (2006) 1696–1702.
[16] C.E. Welty, James R. Wicks, R.E. Wilson, G.L. Rorrer, Fundamentals of Momentum, Heat and Mass Transfer, fifth ed., John Wiley and Sons, 2008.
[17] S.H. Wong, M.C. Ward, C.W. Wharton, Micro T-mixer as a rapid mixing micromixer, Sens. Actuat. B 100 (2004) 359–379.
[18] F. Yan, B. Farouk, Numerical simulation of gas flow and mixing in a microchannel using the direct simulation Monte Carlo method, Microscale Thermophys. Eng. 6 (2002) 235–251.
[19] H. Zhang, M. Xie, DSMC simulation of non-premixed combustion of H_2/O_2 in a Y-shaped microchannel, Nanoscale Microscale Thermophys. Eng. 19 (2015) 31–62.
[20] F. Zhao, T. Armstrong, A. Virkar, Measurement of o2–n2 effective diffusivity in porous media at high temperatures using an electrochemical cell, J. Electrochem. Soc. 150 (2003) A249–A256.